POLISH POLAR RESEARCH
vol. 34, no. 3, pp. 237–252, 2013 doi: 10.2478/popore-2013-0020

Distinguishing between two Antarctic species of Eocene *Palaeeudyptes* penguins: a statistical approach using tarsometatarsi

Piotr JADWISZCZAK[1] and Carolina ACOSTA HOSPITALECHE [2]

[1] *Instytut Biologii, Uniwersytet w Białymstoku, ul. Świerkowa 20B, 15-950 Białystok, Poland <piotrj@uwb.edu.pl>*

[2] *División Paleontología Vertebrados, Museo de La Plata, Paseo del Bosque s/n, B1900FWA, La Plata, Argentina <acostacaro@fcnym.unlp.edu.ar>*

Abstract: Defining species boundaries, due to morphological variation, often represents a significant challenge in paleozoology. In this paper we report results from multi- and univariate data analyses, such as enhanced clustering techniques, principal coordinates ordination method, kernel density estimations and finite mixture model analyses, revealing some morphometric patterns within the Eocene Antarctic representatives of *Palaeeudyptes* penguins. These large-sized birds were represented by two species, *P. gunnari* and *P. klekowskii*, known mainly from numerous isolated bones. Investigations focused on tarsometatarsi, crucial bones in paleontology of early penguins, resulted in a probability-based framework allowing for the "fuzzy" partitioning the studied specimens into two taxa with partly overlapping size distributions. Such a number of species was supported by outcomes from both multi- and univariate studies. In our opinion, more reliance should be placed on the quantitative analysis of form when distinguishing between species within the Antarctic *Palaeeudyptes*.

Key words: Antarctic, La Meseta Formation, Paleogene, Sphenisciformes, statistics, systematics.

Introduction

Penguins (Aves: Sphenisciformes) have the fairly extensive Paleogene fossil record (Jadwiszczak 2009) and their earliest unambiguous remains, assignable to three species, were reported from the Paleocene of New Zealand and the Antarctic Peninsula (Tambussi *et al.* 2005; Slack *et al.* 2006). Eocene penguins were very diversified and widely distributed over the Southern Hemisphere (Clarke *et al.* 2003, 2007, 2010; Jadwiszczak 2006; Tambussi *et al.* 2006; Sallabery *et al.* 2010; Fordyce and Thomas 2011), whereas those from the Oligocene are known from New Zealand

(numerous fossils; Jadwiszczak 2009; Ksepka *et al.* 2012), Australia (Park and Fitzgerald 2012) and Patagonia (Acosta Hospitaleche and Tambussi 2008).

The genus *Palaeeudyptes* is unique among the Paleogene Sphenisciformes and this well-deserved term has its roots in several circumstances, most importantly: (i) it is the earliest erected taxon of fossil penguins (Huxley 1859), (ii) hundreds of remains that have been assigned to this genus are intriguingly widespread, both in space (Antarctica, Australia, New Zealand, South America) and time (Eocene, Oligocene), and (iii) its monophyly has been recently most vigorously contested (*e.g.*, Ksepka *et al.* 2006 and Clarke *et al.* 2007). Type specimens of all but one member species, *i.e. Palaeeudyptes antarcticus* Huxley, 1859 (from New Zealand), *P. gunnari* (Wiman, 1905) and *P. klekowskii* Myrcha, Tatur *et* del Valle, 1990 (both from the Antarctic Peninsula), are isolated tarsometatarsi (hind-limb bones). *P. marplesi* Brodkorb, 1963 (New Zealand penguin) was erected based on the crushed tarsometatarsus and probably associated elements (Brodkorb 1963). The holotype of the type species (*P. antarcticus*) is most probably early Oligocene in age (Ksepka *et al.* 2012), whereas other species are as old as Eocene (*e.g.*, Jadwiszczak 2009). Although great advances has been made in recent years in studies of the above-mentioned taxa (Acosta Hospitaleche and Reguero 2010; Jadwiszczak and Mörs 2011; Jadwiszczak 2012, 2013; Ksepka *et al.* 2012; Acosta Hospitaleche 2013), restricting *Palaeeudyptes* to a monophyletic group of species requires more complete material (*e.g.*, Ksepka *et al.* 2012). Recently, Ksepka *et al.* (2012, p. 251) reasonably suggested to retain them within a single genus in order to avoid highly probable synonymy-related problems in future. Especially, that there is at least one unnamed species, the Burnside Formation "*Palaeeudyptes*" from New Zealand (*e.g.*, Ksepka *et al.* 2012; see also Jadwiszczak 2013), that ought to be taken into account.

In this paper, we report on new data about morphometric patterns in Antarctic *Palaeeudyptes*, a group comprising two closely related and unsatisfactorily delimited (*e.g.*, Jadwiszczak and Mörs 2011) Eocene penguin species. We also evaluate its integrity and offer a preliminary probabilistic method for reasoning on the classification of tarsometatarsi attributable to these early sphenisciforms. Our reasoning is supported by a wide array of statistical techniques.

Geological setting

Seymour (Marambio) Island is located at the Antarctic Peninsula, off the west side of the peninsula's northernmost tip, within the back-arc James Ross Basin (64°17'S, 56°45'W). It is unique in lacking a permanent ice cover. The Eocene La Meseta Formation (Elliot and Trautman 1982) is a fossiliferous lens exposed in the north-eastern part of the island. It comprises deltaic, estuarine and shallow marine siliciclastic sediments, mainly fine-grained and poorly consolidated (Porębski 2000; Marenssi 2006; Tatur *et al.* 2011). The La Meseta Formation yielded the

vast majority of Antarctic fossil penguins including all known bones attributable to either *Palaeeudyptes gunnari* or *P. klekowskii*.

Material and methods

Material. — Antarctic penguin bones discussed here were collected within the Eocene La Meseta Formation on Seymour Island, Antarctic Peninsula and are permanently located at the Museo de La Plata in La Plata (Argentina; abbreviated MLP), the Institute of Biology, University of Białystok (Poland; abbreviated IB/P/B) and the Naturhistoriska riksmuseet in Stockholm (Sweden; abbreviated NRM-PZ). The holotype of *Palaeeudyptes antarcticus* from the Oligocene of New Zealand is housed at the Natural History Museum, London (UK; abbreviated NHMUK). For catalog numbers of all these specimens, see Appendices 1 and 2.

Measurements. — The following tarsometatarsal measurements were taken for this study (numbers of data points for Antarctic *Palaeeudyptes*[1] are after commas): (i) length, 48; (ii) mediolateral width at midshaft, 64; (iii) dorsoplantar thickness at midshaft, 88; (iv) dorsoplantar thickness of proximal end (between intercondylar eminence and hypotarsal sulcus), 38; (v) mediolateral width of trochlea III, 71; (vi) dorsoplantar thickness of trochlea III (along its groove), 71. For more detailed definitions, see Myrcha *et al.* 2002. All measurements were taken with digital calipers and rounded to the nearest 0.1 mm.

Statistical treatment. — Statistical analyses were performed using R language and environment for statistical computing (R Core Team 2013). The hierarchical clustering was conducted by means of the pvclust – an R package that allows for assessing the uncertainty of such grouping (two measures of uncertainty were available; Suzuki and Shimodaira 2006). Here, the recommended AU (Approximately Unbiased) support value, computed by the multiscale bootstrap resampling (10000 replications), was used. The larger the support value (maximally 1 or 100%), the more strongly a given cluster is supported by data. The Ward linkage method (based on minimization of sum of squares, regarded as a very efficient technique) was chosen, which required the squared Euclidean distance as a measure of dissimilarity. Since the latter was not directly implemented in the package, a slightly modified (by PJ) unofficial version of the source code (090824) available from the web page http://www.is.titech.ac.jp/~shimo/prog/pvclust, was utilized. The Principal Coordinates ordination method (PCoA; ape package; Paradis *et al*. 2004) that maps observed dissimilarities (Euclidean distances here) linearly onto a low-dimensional graph and the Minimum Spanning Tree (MST; ape package) were combined to pro-

[1] Tarsometatarsi of debatable taxonomic assignment to *Palaeeudyptes* (see Jadwiszczak 2013) were not included into analyses.

vide additional validation of an output from the above-mentioned clustering procedure. The MST is a minimum-length connected tree comprising a set of straight line segments joining pairs of points (*e.g.*, in a multidimensional space) with no loops and unvisited points (Gower and Ross 1969).

Non-hierarchical clustering was performed by means of a robust method based on the augmented PAM algorithm implemented in the cluster package as the pam function (Maechler *et al.* 2013). PAM stands for the Partitioning Around Medoids, *i.e.* actual objects from the data set found in such a way that the sum of the within cluster dissimilarities is minimized. The silhouette plot and coefficient (a mean of scores across all clusters) were used for validation. The closer to 1 is the latter the more reasonable structure has been found. The lowest acceptable value for a reasonable structure is 0.51. In the case of individual objects/specimens, a silhouette score (width) can vary between -1 and 1. A silhouette value of 1 means that the object is well classified in the cluster, -1 – do not really fits in it, and 0 – most probably lies between clusters. The additional validation was performed via fuzzy clustering (fanny method from the cluster package), which has the advantage that it does not put every object into a specific cluster and its membership coefficients are distributed (most often unevenly, but sum to 1) over a number of groups. Changing the membership exponent, a parameter used in the fit criterion, allows for analyzing behavior of various measures, such as silhouette and Dunn's coefficients, for a given number of clusters. The latter coefficient in its normalized form approaches 1 for a near-crisp clustering.

Procedures here reported were performed using raw, *i.e.* unstandardized, data from the same scale (linear measurements). Since the situation that actually existing clusters are embedded in the unstandardized space is (presumably) not less likely to occur than that considering the rescaled variable space, standardization is not always appropriate prior to the clustering (*e.g.*, Milligan and Cooper 1988). Another important advantage of this approach, at least from our point of view, is that the incorporation of a new object to the analysis does not affect the established distances between any two objects (*e.g.*, Hill and Lewicki 2006). This characteristic, in turn, justifies the addition of the Oligocene New Zealand species, *P. antarcticus*, to the dataset representing differences amidst the Eocene Antarctic taxa (including *P. gunnari* and *P. klekowskii*) and then conducting analyses and some preliminary reasoning in a context of both the morphometric partitioning at the assemblage level (*i.e.*, excluding *P. antarcticus*) and *P. antarcticus* vs. Antarctic *Palaeeudyptes* (dis)similarity issues.

The kernel density estimation (KDE), a non-parametric technique to estimate the probability density function of a random variable, was conducted using the generic density function from the stats package (R Core Team 2013). The Gaussian kernel was chosen and three bandwidth selectors were utilized: classical Silverman's "rule of thumb" (nrd0), Scott (nrd) and Sheather-Jones (SJ) methods. The finite mixture model analyses for univariate data were performed using the normalmixEM function

from the mixtools package (Benaglia *et al.* 2009). This method is based on the iterative expectation–maximization (EM) algorithm (McLachlan and Krishnan 2008). The Penalized Expected Deviance (PED), a useful measure of model complexity and fit was used for additional validation. Models with smaller PED should be preferred to models with larger PED. This measure is available via the density estimation through normal mixtures using the Markov Chain Monte Carlo (MCMC) methodology implemented in the mixAK package as the NMixMCMC function (Komárek 2009). The following parameter values were specified explicitly for the function: priorK = fixed (with Kmax = 2 through 5 for different analyses), burn = 100000, keep = 100000, thin= 10, info= 10000 and PED = TRUE. Ashman's D was used as a measure of meaningfulness of the separation in case of a mixture of two normal distributions (Ashman *et al.* 1994). The analysis of the strength of linear correlation between the trochlear thickness and the bone length was preceded by the visual inspection of the scatterplot and computations, including the randomization test, were performed using the Rundom Pro 3.14 application (created by PJ and available from http://pjadw.lycos.com).

Results

Multivariate analyses. — The hierarchical clustering of 28 well-preserved tarsometatarsi assignable to six genera of Eocene penguins from Seymour Island (and a New Zealand specimen; Appendix 1) revealed two high-level clusters strongly supported by data (AU support values above 95%), but formed at substantially different levels of dissimilarity (Fig. 1A). These were *Anthropornis* + *Palaeeudyptes* vs. other genera. Dissimilarity within the former group was quite well pronounced and, with a single exception (MLP 94-III-15-20; *Palaeeudyptes* located in the *Anthropornis* cluster), was in line with classification at the generic level. Moreover, the existence of two equally numerous (n = 8) and supported (AU value = 82%) sets within *Palaeeudyptes* appears to be conspicuous (Fig. 1A, Appendix 1). The prevalence of specimens attributable to *P. klekowskii* within the rightmost cluster (edge 21) and those assignable to *P. gunnari* within its left-sided neighbor (edge 20), is noteworthy. The type specimen of *Palaeeudyptes antarcticus* from New Zealand (NHMUK A1048) most closely resembled (at least morphometrically) the specimen MLP 91-II-4-222 (*P. gunnari* in Myrcha *et al.* 2002; AU-value = 100%) from Seymour Island. Standard errors for high AU-values were negligible (Fig. 1B). The minimum spanning tree based on principal coordinates generally confirmed the adequacy of the clusters, but highlighted the somewhat fuzzy delimitation within the *Palaeeudyptes* group (Fig. 2).

The partitioning around four medoids perfectly recreated the cluster membership assigned by means of the hierarchical clustering (Fig. 3A, Appendix 1). Such a number of medoids (four) was enforced to account for results from the previous

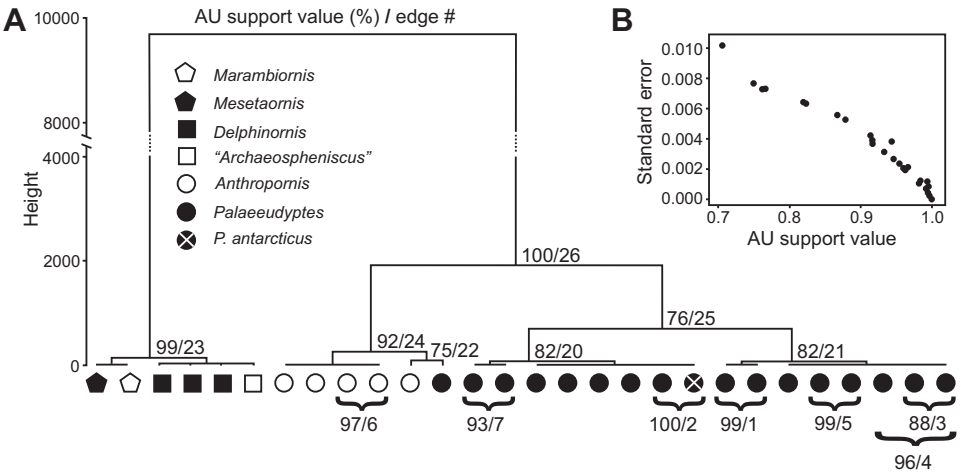

Fig. 1. Hierarchical partitioning the Eocene Antarctic penguins (plus the Early Oligocene *P. antarcticus* from New Zealand) based on squared Euclidean distances and the Ward linkage. Dendrogram with resampling-based support values (**A**) and standard error decay for the latter (**B**). More details in text and Appendix 1.

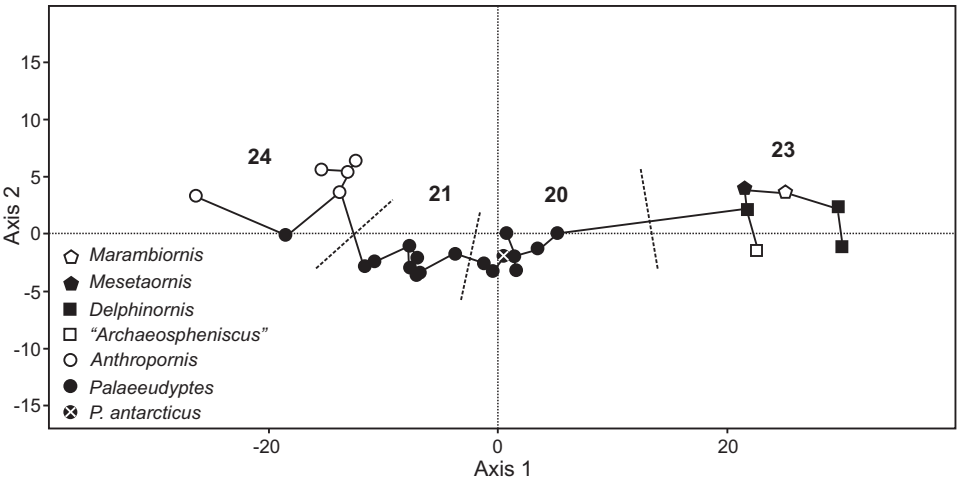

Fig. 2. Principal Coordinates Analysis of the Eocene Antarctic penguins and the early Oligocene *P. antarcticus* from New Zealand with the superimposed minimum spanning tree. First two axes shown. Numbers above groups of symbols denote edge numbers from Fig. 1.

analysis. Moreover, results from validation via the fuzzy clustering testified that this was the most reasonable choice (Fig. 4). The medoids for the respective clusters (see Fig. 3A) were as follows: cluster no. 1, MLP 94-III-15-345 (*Palaeeudyptes* sp.); no. 2, MLP 91-II-4-222 (*Palaeeudyptes gunnari*); no. 3, MLP 96-I-6-19 (*Anthropornis*) and no. 4, IB/P/B-0490 (*Marambiornis exilis*). The lowest within-cluster silhouette scores (*i.e.*, the worst matching) were assigned to: cluster no. 1, MLP 84-II-1-78

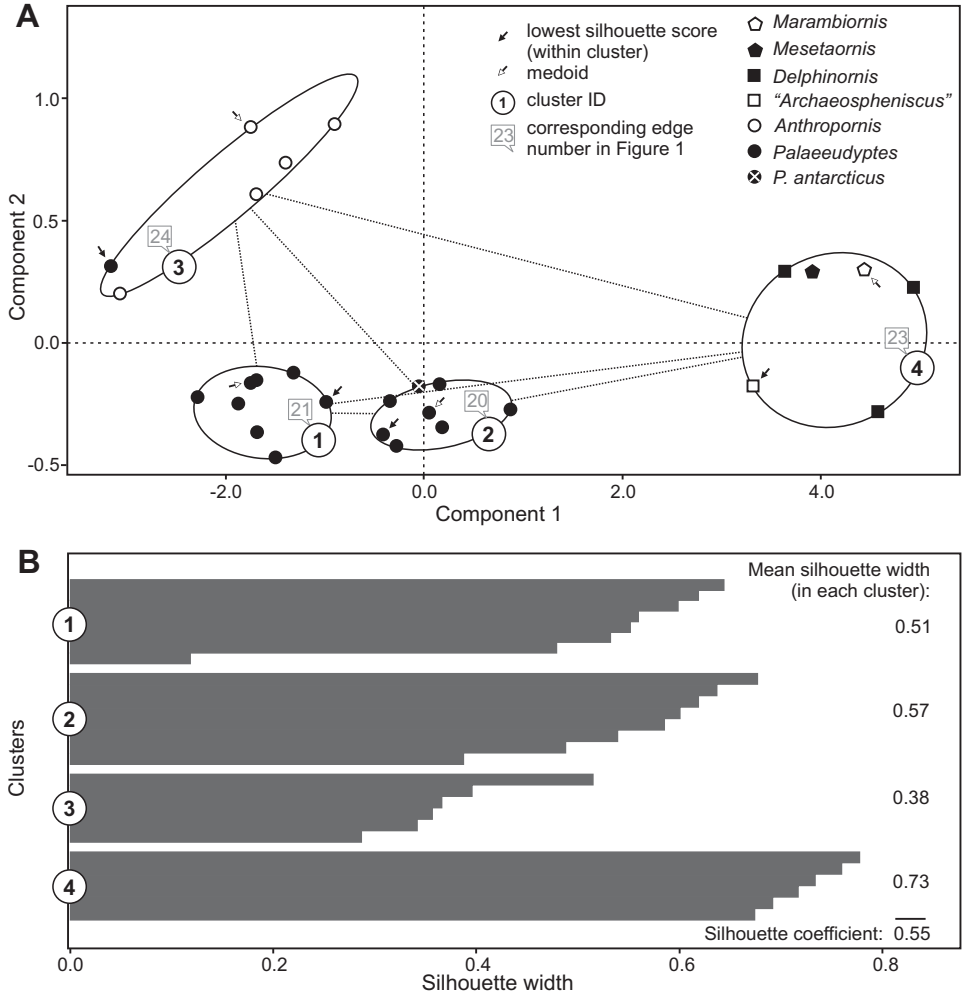

Fig. 3. Non-hierarchical clustering using partitioning around medoids the Eocene Antarctic penguins (plus the Early Oligocene *P. antarcticus* from New Zealand). Clusters with data presented in the context of the Principal Component Analysis (**A**) and the silhouette plot (**B**). More details in text.

(*Palaeeudyptes klekowskii*); no. 2, IB/P/B-0552 (*Palaeeudyptes* sp.); no. 3, MLP 94-III-15-20 (*Palaeeudyptes klekowskii*); and no. 4, MLP 90-I-20-24 ("*Archaeospheniscus*" *wimani*). None of them was negative, though (see also Fig. 3). The cluster no. 4 (including four genera: "*Archaeospheniscus*", *Delphinornis*, *Marambiornis* and *Mesetaornis*) was most strongly supported by data (mean silhouette width of 0.73; Fig. 3B), whereas the cluster no. 3 was the weakest one (mean silhouette width of 0.38; Fig. 3B). The value of the silhouette coefficient (0.55) allowed for reporting the existence of a reasonable structure with three well-supported clusters: 1, 2 and 4 (see Material and methods and Fig. 3B). The first set, however, included a single object (MLP 84-II-1-78, *P. klekowskii*) that is very poorly classified in it and most

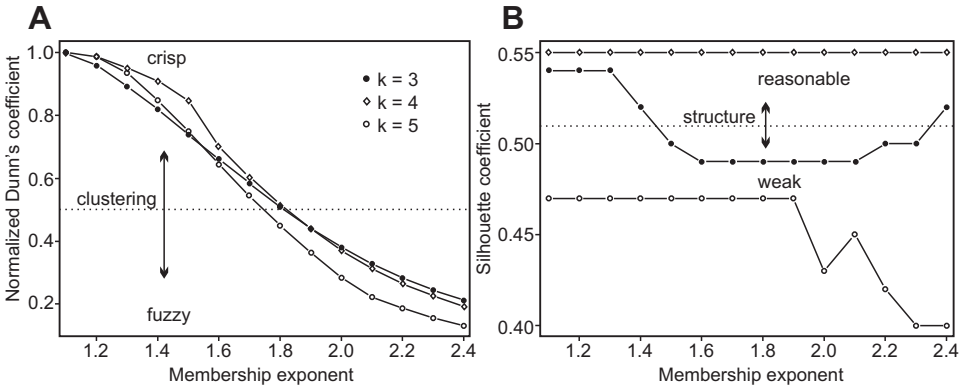

Fig. 4. Stability of three models of partitioning the Eocene Antarctic penguins (plus the Early Oligocene *P. antarcticus* from New Zealand) for different levels of membership exponent, a parameter of the fuzzy clustering used in the fit criterion. Model response is expressed in terms of changes in values of Dunn's coefficient (**A**) and silhouette coefficient (**B**). More details in text.

likely was lying between clusters no. 1 and 2 (score close to 0; see Material and methods and Fig. 3B).

Univariate analyses. — The dorsoplantar thickness of the trochlea III was the only linear measurement taken from tarsometatarsi assignable to Antarctic *Palaeeudyptes* (see Material and methods) that both provided a sample of reasonable size (n = 71; Appendix 2) and exhibited clear signs of bimodality. The estimated Gaussian kernel density for three different bandwidths (see Material and methods) resulted in a curve resembling that for the normal probability density function fitted except its central portion (Fig. 5A). The pronounced flatness of this part was reflected numerically in the sample excess kurtosis (K = -0.586). The bandwidth chosen using Silverman's selector most clearly suggested the existence of bimodality (Fig. 5A) and the latter was also conspicuous in histograms (not presented in this work). Moreover, the normal-mixture estimation using Markov Chain Monte Carlo yielded the lowest penalized expected deviance for a two-component case (Table 1). The finite mixture analysis resulted in two sets of parameters (*i.e.*, means and standard deviations; Fig. 5B) of normal density functions with

Table 1

Output from the normal mixture exploration using the Markov Chain Monte Carlo method applied to the dorsoplantar thickness of the tarsometatarsal trochlea III (for details, see Material and methods). k stands for the number of components.

k	Expected Deviance	Optimism	Penalized Expected Deviance
2	293.686	20.720	314.405
3	294.474	26.261	320.735
4	292.864	28.331	321.195
5	292.597	33.750	326.347

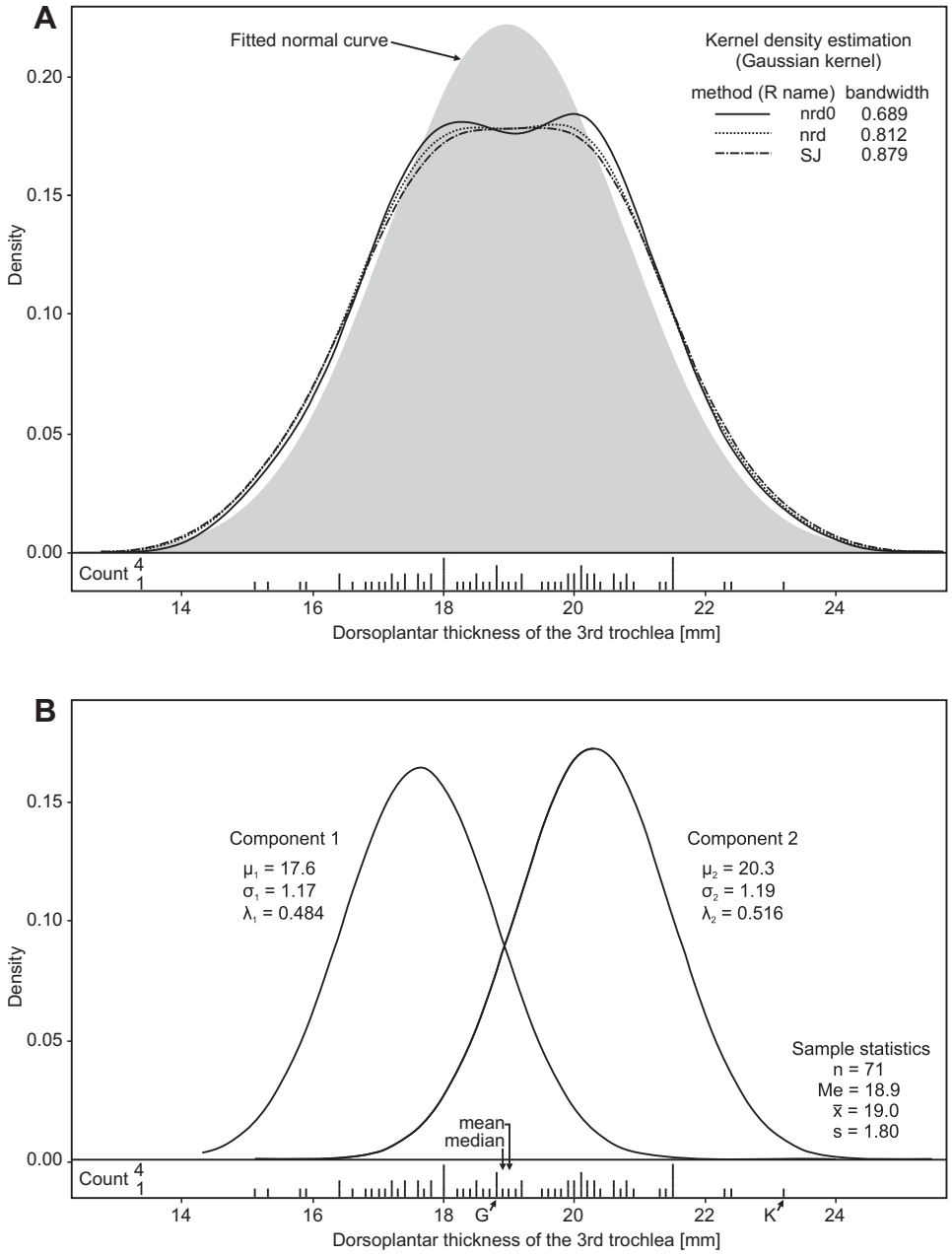

Fig. 5. Kernel density estimation using Gaussian kernel and three bandwidth selectors for the trochlear thickness of the Antarctic *Palaeeudyptes* penguins (**A**) and results of the finite normal mixture model analysis (**B**). Each of two density components from the latter plot was scaled by the estimated probablility of an observation being drawn from that component distribution. Abbreviations: G – holotype of *Palaeeudyptes gunnari*, K – holotype of *P. klekowskii*, λ – local estimate of the mixing proportions. For details, see text and Appendix 2.

similar local estimates of the mixing proportions for the inputted data (λ; Fig. 5B). Ashman's D for these values was 2.288. Since bones attributed to *Palaeeudyptes klekowskii* are traditionally regarded as larger than those of its only Antarctic congeneric (*e.g.,* Myrcha *et al.* 2002), Component 1 and Component 2 in Fig. 5B correspond to density functions for *P. gunnari* and *P. klekowskii*, respectively. For posterior probabilities for observations, values of the trochlear thickness, see Appendix 2. The linear relationship between the trochlear thickness and the bone length in *Palaeeudyptes* was very strong (Pearsonian r = 0.87) and statistically significant (n = 40, 10000 randomizations, $P_{two\text{-}sided} = 0.0001$).

Discussion and conclusions

The basic pattern resulting from the hierarchical partitioning agreed in its topology (Fig. 1A) with the shape of phylogenetic trees recently reported for the Eocene Antarctic penguins (Jadwiszczak 2013; see also Ksepka *et al.* 2012). In both cases *Palaeeudyptes* formed either a clade or a cluster solely with *Anthropornis*. Relatively low, in the case of adopting the 95% cutoff level, support values computed for both *Palaeeudyptes*-only clusters (82%) most probably reflect the high level of intrageneric variability, partly resulting from the overlapping size distributions of member species (Fig. 5). Additionally, the shape of the combined distribution differs across measurement categories, which can further affect the partitioning. The Ward linkage method used for the hierarchical clustering tends to create clusters of small size (Hill and Lewicki 2006). It appears not to be an issue in our analyses, though (Fig. 1A).

The persisting position of *Palaeeudyptes antarcticus* from New Zealand within the set of bones traditionally attributable to *P. gunnari* (Figs 1–3, Appendix 1), smaller of two Antarctic *Palaeeudyptes* species (Myrcha *et al.* 2002), is noteworthy. Anyway, we are convinced that any categorical statements considering their close phylogenetic affinity, based solely on numerical data, would be too far-going. As the holotype of *P. antarcticus* (NHMUK A1048) is an incomplete and isolated bone (Huxley 1859; Jadwiszczak 2009, fig. 1) of debatable age (*e.g.*, Ksepka *et al.* 2012), a conclusive phylogenetic analysis should await discoveries of more complete fossils. On the other hand, the existence of a clear similarity between these New Zealand and Antarctic specimens that had prompted Simpson (1971) to revise the taxonomical position of *Eosphaeniscus gunnari* Wiman, 1905, has gained some numerical support here.

A single specimen (MLP 94-III-15-20) assignable, based on diagnostic features, to *Palaeeudyptes klekowskii* (Myrcha *et al.* 2002), but located by partitioning algorithms within *Anthropornis* (Figs 1–3), is the largest tarsometatarsus from the former genus ever reported. As it forms a two-specimen cluster with the largest foot bone attributable to *Anthropornis* (MLP 94-III-15-356; Fig. 1A), it seems reasonable to explain this interesting linkage in terms of size-related constraints af-

fecting bone proportions. Moreover, despite remarks above, MLP 94-III-15-20 is, in context of PAM partitioning, the most poorly matching tarsometatarsus within the *Anthropornis* cluster (Fig. 3).

Because of their unsatisfactory preservation, type specimens of *Palaeeudyptes gunnari* and *P. klekowskii* (NRM-PZ A7 and IB/P/B-0065; Wiman 1905; Simpson 1971 and Myrcha *et al.* 1990) could not be included into multivariate analyses. The only univariate analysis that revealed the clear bimodality (Ashman's $D > 2$; see also Fig. 5A) in the investigated data set identified the former bone as a very typical one, whereas the latter – as the most extreme specimen among measured tarsometatarsi (Fig. 5B). In other words, NRM-PZ A7 has similar posterior probabilities as a member of the set modeled by Component 1 (corresponding to *P. gunnari*) and Component 2 (*P. klekowskii*) (Appendix 2). Since it is also quite heavily abraded, its usefulness as a type specimen is limited. The specimen IB/P/B-0065 is almost certainly a member of the set modeled by Component 2 and its posterior probability in the context of Component 1 is below 0.001 (Fig. 5, Appendix 2). This holotype, although incomplete, is less abraded than the former specimen, and in contrast to it, paratypes were formally designated (Myrcha *et al.* 1990; see also Simpson 1971; Myrcha *et al.* 2002; Jadwiszczak 2006). The extreme position of the above-mentioned bone within the empirical distribution ought to be taken into account in future comparisons.

Estimates of the mixing proportions (λ; Fig. 5B) suggest that both taxa of these large-sized Eocene penguins could have been almost equally numerous. This finding is very close to the ratio 48:52 resulting from data reported by Myrcha *et al.* (2002, pp. 22, 24). The median for the distribution of trochlear thickness values (18.9; Fig. 5B) corresponds to posterior probablilities of 0.51 and 0.49 for Component 1 and 2, respectively (Appendix 2). Although the existence of the skeletal sexual size dimorphism (SSD) within these birds is probable (Jadwiszczak and Mörs 2011), and is present in their extant counterparts (Livezey 1989), its magnitude cannot be assessed. New specimens affected the range of available data points making the SSD less feasible. Moreover, the correlation between the trochlear thickness and the tarsometatarsal length (the latter measure was used by Jadwiszczak and Mörs [2011]), although strong and statistically significant (see Results), is not the perfect one. The obtained value, expressed in terms of the coefficient of determination (r^2), means that 76% of the tarsometatarsal length is directly accounted for by the trochlear thickness and vice versa. This result should be interpreted as a warning against too far-going interpretations of single measures and justifies the probability-based considerations. For example, the specimen IB/P/B-0065 (*i.e.*, holotype of *P. klekowskii*) is 6.6% shorter than the longest tarsometatarsus assigned to *Palaeeudyptes* (MLP 94-III-15-20) while having the larger (7.3%) trochlea III. The posterior probability that the latter is a member of the set modeled by Component 2 (corresponding to *P. klekowskii*; Fig. 5B) remains impressively high (0.99). Anyway, we followed a more traditional approach here, assuming the predominantly phylogeny-related origin of the observed *scope* of variability.

To conclude, the presence of the morphometric heterogeneity within studied tarsometatarsi of *Paleeudyptes* penguins from Antarctica, regardless its roots, appears to be a real phenomenon. Results presented above allow for a preliminary insight into its form and provide some framework for uncertainty quantification (using probabilities) in specimen-classification considerations. In our opinion, more reliance should be placed on morphometric differences, combined with the analysis of purely qualitative traits, when distinguishing between species within the Antarctic *Palaeeudyptes*.

Acknowledgements. — We are indebted to Mieczysław Wolsan (Warszawa) and Martin Chávez Hoffmeister (Bristol) for helpful reviews. The first author appreciates the financial support through SYNTHESYS funding made available by the European Community – Research Infrastructure Action under the FP6 and FP7 "Structuring the European Research Area" Programme; projects SETAF-4399 and GBTAF-987 respectively.

References

ACOSTA HOSPITALECHE C. 2013. *Palaeeudyptes klekowskii* Myrcha, Tatur y del Valle, 1990: descripción e importancia del más completo esqueleto de pingüino del Eoceno superior de Antártida. *27° Jornadas Argentinas de Paleontología de Vertebrados (La Rioja, Argentina). Actas*: 14.

ACOSTA HOSPITALECHE C. and REGUERO M. 2010. First articulated skeleton of *Palaeeudyptes gunnari* from the late Eocene of Seymour (= Marambio) Island (Antarctica). *Antarctic Science* 22: 289–298.

ACOSTA HOSPITALECHE C. and TAMBUSSI C. 2008. South American fossil penguins: a systematic update. *Oryctos* 7: 109–127.

ASHMAN K.M., BIRD C.M. and ZEPF S.E. 1994. Detecting bimodality in astronomical datasets. *Astronomical Journal* 108: 2348.

BENAGLIA T., CHAUVEAU D., HUNTER D.R. and YOUNG D. 2009. Mixtools: An R package for analyzing finite mixture models. *Journal of Statistical Software* 32: 1–29.

BRODKORB P. 1963. Catalogue of fossil birds. *Bulletin of the Florida State Museum* 7: 179–293.

CLARKE J.A., OLIVERO E.B. and PUERTA P. 2003. Description of the earliest fossil penguin from South America and first Paleogene vertebrate locality of Tierra del Fuego, Argentina. *American Museum Novitates* 3423: 1–18.

CLARKE J.A., KSEPKA D.T., STUCCHI M., URBINA M., GIANNINI N., BERTELLI S., NARVÁEZ Y. and BOYD C.A. 2007. Paleogene equatorial penguins challenge the proposed relationship between biogeography, diversity, and Cenozoic climate change. *Proceedings of the National Academy of Sciences (PNAS)* 104: 11545–11550.

CLARKE J.A., KSEPKA D.T., SALAS-GISMONDI R., ALTAMIRANO A.J., SHAWKEY M.D., D'ALBA L., VINTHER J., DEVRIES T.J. and BABY P. 2010. Fossil Evidence for Evolution of the Shape and Color of Penguin Feathers. *Science* 330: 954–957.

ELLIOT D.H. and TRAUTMAN T.A. 1982. Lower Tertiary strata on Seymour Island, Antarctic Peninsula. *In*: C. Craddock (ed.) *Antarctic Geoscience*. The University of Wisconsin Press, Madison: 287–297.

FORDYCE R.E. and THOMAS D.B. 2011. *Kaiika maxwelli*, a new early Eocene archaic penguin (Sphenisciformes, Aves) from Waihao Valley, South Canterbury, New Zealand. *New Zealand Journal of Geology and Geophysics* 54: 43–51.

GOWER J.C. and ROSS G.J.S. 1969. Minimum Spanning Trees and Single Linkage Cluster Analysis. *Journal of the Royal Statistical Society, Series C (Applied Statistics)* 18: 54–64.

HILL T. and LEWICKI P. 2006. *Statistics: methods and applications: a comprehensive reference for science, industry, and data mining*. StatSoft, Inc., Tulsa: 832 pp.

HUXLEY T.H. 1859. On a fossil bird and a fossil cetacean from New Zealand. *Quarterly Journal of the Geological Society of London* 15: 670–677.

JADWISZCZAK P. 2006. Eocene penguins of Seymour Island, Antarctica: Taxonomy. *Polish Polar Research* 27: 3–62.

JADWISZCZAK P. 2009. Penguin past: The current state of knowledge. *Polish Polar Research* 30: 3–28.

JADWISZCZAK P. 2012. Partial limb skeleton of a "giant penguin" *Anthropornis* from the Eocene of Antarctic Peninsula. *Polish Polar Research* 33: 259–274.

JADWISZCZAK P. 2013. Taxonomic diversity of Eocene Antarctic penguins: a changing picture. *In:* M.J. Hambrey, P.F. Barker, P.J. Barrett, V. Bowman, B. Davies, J.L. Smellie and M. Tranter (eds) *Antarctic Palaeoenvironments and Earth-Surface Processes*. Geological Society (London), Special Publications 381. First published online June 25, 2013, http://dx.doi.org/10.1144/SP381.7.

JADWISZCZAK P. and MÖRS T. 2011. Aspects of diversity in early Antarctic Penguins. *Acta Palaeontologica Polonica* 56: 269–277.

KOMÁREK A. 2009. A new R package for Bayesian estimation of multivariate normal mixtures allowing for selection of the number of components and interval-censored data. *Computational Statistics and Data Analysis* 53: 3932–3947.

KSEPKA D.T., BERTELLI S. and GIANNINI N.P. 2006. The phylogeny of the living and fossil Sphenisciformes (penguins). *Cladistics* 22: 412–441.

KSEPKA D.T., FORDYCE R.E., ANDO T. and JONES C.M. 2012. New fossil penguins (Aves, Sphenisciformes) from the Oligocene of New Zealand reveal the skeletal plan of stem penguins. *Journal of Vertebrate Paleontology* 32: 235–254.

LIVEZEY B.C. 1989. Morphometric patterns in Recent and fossil penguins (Aves, Sphenisciformes). *Journal of Zoology* (London) 219: 269–307.

MAECHLER M., ROUSSEEUW P., STRUYF A., HUBERT M. and HORNIK K. 2013. Cluster: Cluster analysis basics and extensions. R package (version 1.14.4) available from http://cran.r-project.org/web/packages/cluster.

MARENSSI S.A. 2006. Eustatically controlled sedimentation recorded by Eocene strata of the James Ross Basin, Antarctica. *In*: J.E. Francis, D. Pirrie and J.A. Crame (eds) Cretaceous–Tertiary High-Latitude Palaeoenvironments, James Ross Basin, Antarctica. *Geological Society, London Special Publications* 258: 125–133.

MCLACHLAN G. and KRISHNAN T. 2008. *The EM Algorithm and Extensions. 2nd edition*. John Wiley & Sons, Inc., Hoboken: 400 pp.

MILLIGAN G.W. and COOPER M.C. 1988. A study of standardization of variables in cluster analysis. *Journal of Classification* 5: 181–204.

MYRCHA A., JADWISZCZAK P., TAMBUSSI C.P., NORIEGA J.I., GAŹDZICKI A., TATUR A. and DEL VALLE R. 2002. Taxonomic revision of Eocene Antarctic penguins based on tarsometatarsal morphology. *Polish Polar Research* 23: 5–46.

MYRCHA A., TATUR A. and DEL VALLE R.A. 1990. A new species of fossil penguin from Seymour Island, West Antarctica. *Alcheringa* 14: 195–205.

PARADIS E., CLAUDE J. and STRIMMER K. 2004. APE: analyses of phylogenetics and evolution in R language. *Bioinformatics* 20: 289–290.

PARK T. and FITZGERALD E.M.G. 2012. A review of Australian fossil penguins (Aves: Sphenisciformes). *Memoirs of Museum Victoria* 69: 309–325.

PORĘBSKI S.J. 2000. Shelf-valley compound fill produced by fault subsidence and eustatic sea-level changes, Eocene La Meseta Formation, Seymour Island, Antarctica. *Geology* 28: 147–150.

R CORE TEAM 2013. *R: A language and environment for statistical computing*. R Foundation for Statistical Computing, Vienna, Austria. URL http://www.R-project.org.

SALLABERRY M.A., YURY-YÁÑEZ R.E., OTERO R.A., SOTO-ACUÑA S. and TORRES T. 2010. Eocene birds from the western margin of southernmost South America. *Journal of Paleontology* 84: 1061–1070.

SIMPSON G.G. 1971. Review of fossil penguins from Seymour Island. Proceedings of the *Royal Society of London B* 178: 357–387.

SLACK K.E., JONES C.M., ANDO T., HARRISON G.L., FORDYCE R.E., ARNASON U. and PENNY D. 2006. Early penguin fossils, plus mitochondrial genomes, calibrate avian evolution. *Molecular Biology and Evolution* 23: 1144–1155.

SUZUKI R. and SHIMODAIRA H. 2006. Pvclust: an R package for assessing the uncertainty in hierarchical clustering. *Bioinformatics* 22: 1540–1542.

TAMBUSSI C.P., ACOSTA HOSPITALECHE C.I., REGUERO M.A. and MARENSSI S.A. 2006. Late Eocene penguins from West Antarctica: systematics and biostratigraphy. *In*: J.E. Francis, D. Pirrie and J.A. Crame (eds) *Cretaceous–Tertiary High-Latitude Palaeoenvironments, James Ross Basin, Antarctica*. Geological Society, London, Special Publications 258: 145–161.

TAMBUSSI C.P., REGUERO M.A., MARENSSI S.A. and SANTILLANA S.N. 2005. *Crossvallia unienwillia*, a new Spheniscidae (Sphenisciformes, Aves) from the Late Paleocene of Antarctica. *Geobios* 38: 667–675.

TATUR A., KRAJEWSKI K.P. and DEL VALLE R.A. 2011. The facies and biota of the oldest exposed strata of the Eocene La Meseta Formation (Seymour Island, Antarctica). Geological Quarterly 55: 345–360.

WIMAN C. 1905. Über die alttertiären Vertebraten der Seymourinsel. *Wissenschaftliche Ergebnisse der Schwedischen Südpolar-Expedition 1901–1903* 3: 1–37.

Received 12 July 2013
Accepted 12 August 2013

Appendix 1

Specimens used in the multivariate analyses and four clusters resulting from the Ward hierarchical clustering and partitioning around medoids (for details, see text and Figs 1, 3). The order of edges (and their ID numbers) and specimens within clusters correspond to those in Fig. 1 (read from left to right). Corresponding cluster ID numbers from Fig. 3 are in parentheses. Species assignments are after Myrcha *et al.* (2002).

Edge #23 (4): IB/P/B-484 (*Delphinornis arctowskii*), IB/P/B-0279a (*Delphinornis gracilis*), MLP 90-I-20-24 (*Archaeospheniscus wimani*), IB/P/B-0490 (*Marambiornis exilis*), IB/P/B-0062 (*Delphinornis larseni*), IB/P/B-0278 (*Mesetaornis polaris*).

Edge #24 (3): MLP 95-I-10-142, MLP 94-III-15-356b, MLP 96-I-6-19, MLP 94-III-15-178, MLP 94-III-15-356 (*Anthropornis* sp.), MLP 94-III-15-20 (*Palaeeudyptes klekowskii*).

Edge #20 (2): MLP 94-III-15-16, IB/P/B-0487 (*Palaeeudyptes gunnari*), MLP ---, IB/P/B-0552 (*Palaeeudyptes* sp.), IB/P/B-0072, MLP 87-II-1-45, MLP 91-II-4-222 (*Palaeeudyptes gunnari*), NHMUK A1048 (*Palaeeudyptes antarcticus* from New Zealand).

Edge #21 (1): MLP 83-V-30-15 (*Palaeeudyptes klekowskii*), IB/P/B-0551 (*Palaeeudyptes* sp.), MLP 83-V-30-16, IB/P/B-0485, MLP 84-II-1-78, MLP 84-II-1-124, MLP 93-X-1-63 (*Palaeeudyptes klekowskii*), MLP 94-III-15-345 (*Palaeeudyptes* sp.).

Appendix 2

Posterior probabilities for trochlear dorsoplantar thickness of tarsometatarsi assignable to *Palaeeudyptes* from Seymour Island returned by normalmixEM procedure (mixtools package, R environment). For details, see text and Fig. 5B.

	ID	Trochlear thickness	Posterior probabilities for observations	
			Component 1	Component 2
1	MLP 08-XI-30-15/22	15.1	0.9992	0.0008
2	IB/P/B-0294	15.3	0.9988	0.0012
3	MLP 96-I-6-13	15.8	0.9971	0.0029
4	MLP 93-X-1-84	15.9	0.9965	0.0035
5	MLP 94-III-15-16	16.4	0.9913	0.0087
6	MLP 84-II-1-125	16.4	0.9913	0.0087
7	MLP 94-III-15-339	16.6	0.9874	0.0126
8	IB/P/B-0980	16.8	0.9818	0.0182
9	MLP 93-X-1-151	16.9	0.9781	0.0219
10	MLP 96-I-6-33/35	17.0	0.9737	0.0263
11	MLP 91-II-4-222	17.1	0.9685	0.0315
12	IB/P/B-0487	17.2	0.9623	0.0377
13	MLP 84-II-1-75	17.2	0.9623	0.0377
14	MLP 87-II-1-45	17.3	0.9549	0.0451
15	MLP 95-I-10-16	17.4	0.9461	0.0539
16	MLP 90-I-20-314	17.4	0.9461	0.0539
17	IB/P/B-0112	17.6	0.9234	0.0766
18	IB/P/B-0277	17.6	0.9234	0.0766
19	IB/P/B-0061	17.7	0.9090	0.0910
20	MLP 84-II-1-47	17.8	0.8922	0.1078
21	NHMUK A3341	17.8	0.8922	0.1078
22	MLP 93-X-1-117	18.0	0.8502	0.1498
23	MLP 11-II-20-35	18.0	0.8502	0.1498
24	IB/P/B-0072	18.0	0.8502	0.1498
25	NHMUK A5581	18.0	0.8502	0.1498
26	83-V-20-9	18.2	0.7955	0.2045
27	MLP ---	18.3	0.7630	0.2370
28	MLP 93-X-1-106	18.4	0.7270	0.2730
29	MLP 87-II-1-97	18.5	0.6878	0.3122
30	MLP 94-III-15-179	18.5	0.6878	0.3122
31	MLP 84-II-1-6	18.6	0.6457	0.3543
32	IB/P/B-0553	18.7	0.6011	0.3989
33	MLP 94-III-15-398	18.8	0.5548	0.4452
34	MLP 11-II-20-07	18.8	0.5548	0.4452
35	NHRM-PZ A7	18.8	0.5548	0.4452

	ID	Trochlear thickness	Posterior probabilities for observations	
			Component 1	Component 2
36	IB/P/B-0552	18.9	0.5074	0.4926
37	IB/P/B-0101	19.0	0.4598	0.5402
38	MLP 84-II-1-78	19.1	0.4129	0.5871
39	MLP 83-V-30-16	19.2	0.3675	0.6325
40	MLP 93-X-1-120	19.2	0.3675	0.6325
41	MLP 82-IV-23-5	19.5	0.2465	0.7535
42	MLP 94-III-15-345	19.6	0.2126	0.7874
43	MLP 94-III-15-18	19.7	0.1822	0.8178
44	MLP 84-II-1-76	19.8	0.1553	0.8447
45	MLP 94-III-15-4	19.9	0.1317	0.8683
46	IB/P/B-0556	19.9	0.1317	0.8683
47	MLP 93-X-1-25	20.0	0.1112	0.8888
48	IB/P/B-0546	20.0	0.1112	0.8888
49	MLP 93-X-1-63	20.1	0.0935	0.9065
50	MLP 84-II-1-49	20.1	0.0935	0.9065
51	MLP 93-X-1-65	20.1	0.0935	0.9065
52	MLP 08-XI-30-15/22	20.2	0.0784	0.9216
53	MLP 96-I-6-30/31	20.2	0.0784	0.9216
54	MLP 83-V-30-15	20.3	0.0655	0.9345
55	IB/P/B-0485	20.3	0.0655	0.9345
56	MLP 11-II-20-14	20.4	0.0546	0.9454
57	84-II-1-124	20.6	0.0377	0.9623
58	IB/P/B-0276	20.6	0.0377	0.9623
59	IB/P/B-0093	20.7	0.0313	0.9687
60	MLP 83-V-20-42	20.8	0.0259	0.9741
61	IB/P/B-0555	20.8	0.0259	0.9741
62	IB/P/B-0551	20.9	0.0214	0.9786
63	MLP 93-X-1-6	21.3	0.0099	0.9901
64	IB/P/B-0292	21.4	0.0082	0.9918
65	MLP 94-III-15-20	21.5	0.0067	0.9933
66	MLP 94-III-15-343	21.5	0.0067	0.9933
67	IB/P/B-0281	21.5	0.0067	0.9933
68	IB/P/B-0486	21.5	0.0067	0.9933
69	IB/P/B-0545	22.3	0.0014	0.9986
70	IB/P/B-0142	22.4	0.0012	0.9988
71	IB/P/B-0065	23.2	0.0002	0.9998